HHS Public Access

Author manuscript

J Neurochem. Author manuscript; available in PMC 2018 March 01.

Published in final edited form as:

J Neurochem. 2017 March ; 140(6): 889–902. doi:10.1111/jnc.13749.

Alternate promoter usage generates two subpopulations of the neuronal RhoGEF Kalirin-7

Megan B. Miller[1], **Yan Yan**[1], **Yi Wu**[2], **Bing Hao**[3], **Richard E. Mains**[1], and **Betty A. Eipper**[1,3,*]

[1]Department of Neuroscience, University of Connecticut Health Center, Farmington CT 06030-3401

[2]Center for Cell Analysis and Modeling, University of Connecticut Health Center, Farmington CT 06030-3401

[3]Department of Molecular Biology and Biophysics, University of Connecticut Health Center, Farmington CT 06030-3401

Abstract

Kalirin (Kal), a dual Rho GDP/GTP exchange factor (GEF), plays essential roles within and outside the nervous system. Tissue-specific, developmentally regulated alternative splicing generates isoforms with one (Kal7) or two (Kal9, Kal12) GEF domains along with a kinase (Kal12) domain; while Kal9 and Kal12 are crucial for neurite outgrowth, Kal7 plays important roles in spine maintenance and synaptic plasticity. Tissue-specific usage of alternate *Kalrn* promoters (A, B, C, D) places four different peptides before the Sec14 domain. cSec14, with an amphipathic helix encoded by the C-promoter (Kal-C-helix), is the only variant known to interact with phosphoinositides. We sought to elucidate the biological significance of Kalirin promoter usage and lipid binding. While Ex1B expression was predominant early in development, Ex1C expression increased when synaptogenesis occurred. Kal-C-helix-containing Kal7 (cKal7) was enriched at the PSD, present in the microsomal fraction and absent from cytosol; no significant amount of cKal9 or cKal12 could be identified in mouse brain. Similarly, in primary hippocampal neurons, endogenous cKalirin colocalized with PSD95 in dendritic spines, juxtaposed to Vglut1-positive puncta. When expressed in young neurons, bSec14-EGFP was diffusely distributed, while cSec14-EGFP localized to internal puncta. Transfected bKal7-EGFP and cKal7-EGFP localized to dendritic spines and increased spine density in more mature cultured neurons. Although promoter usage did not alter the Rac-GEF activity of Kal7, the synaptic puncta formed by cKal7-EGFP were smaller than those formed by bKal7-EGFP. Molecular modeling predicted a role for Kal-C-helix residue Arg[15] in the interaction of cSec14 with phosphoinositides. Consistent with this prediction,

*Correspondence: eipper@uchc.edu 860-679-8898; fax 860-679-1885.

Author Contributions

M.B.M. conducted most of the experiments and analyzed data
Y.Y. plated and transfected neuronal cultures
Y.W. designed and validated the Rac1 biosensor and provided extensive technical advice
B.H. carried out the three-dimensional modeling of cSec14
B.A.E. developed the Kal-C-Helix antibody and subcellular fractionation protocols
R.E.M. developed expression vectors, long-range PCR protocols and analyzed promoter information
M.B.M., R.E.M. and B.A.E. jointly designed and analyzed experiments and wrote the manuscript

Conflict of Interest

The authors declare no conflict of interest.

mutation of Arg^{15} to Gln altered the localization of cSec14-EGFP and cKal7-EGFP. These data suggest that phosphoinositide-dependent interactions unique to cKal7 contribute to protein localization and function.

Introduction

Through developmentally regulated alternative splicing, the *Kalrn* gene encodes three major isoforms, Kal7, Kal9 and Kal12, which share a common GDP/GTP exchange factor (GEF) domain specific for Rac1 and RhoG (Fig.1A). Both longer isoforms are expressed in the brain throughout development, with significant expression in muscle, heart, bone and other tissues (Yan *et al.* 2014, Mandela *et al.* 2012, Wu *et al.* 2013, Huang *et al.* 2014, Yan *et al.* 2016). Kal9 and Kal12 are crucial for normal neurite outgrowth and branching. Kal7 expression is limited to the nervous system, and the protein is largely localized to the postsynaptic density (PSD). In rodents, expression of Kal7 begins when synaptogenesis starts.

Through its GEF activity and its non-catalytic domains, Kal7 promotes actin polymerization and structural plasticity in spines. It engages in direct interactions with multiple synaptic proteins, including PSD95 and GluN2B (Penzes *et al.* 2001b, Penzes *et al.* 2003, Ma *et al.* 2008a, Lemtiri-Chlieh *et al.* 2011, Kiraly *et al.* 2011a). As such, Kal7 plays a crucial role in synaptic structure and function. Genetic ablation of Kal7 ($Kal7^{KO}$) results in decreased spine density and substantially impaired structural and functional plasticity (Ma *et al.* 2008a, Lemtiri-Chlieh *et al.* 2011, Lu *et al.* 2015). Behaviorally, $Kal7^{KO}$ animals display impaired fear learning and decreased anxiety-like behavior, as well as increased locomotor sensitivity to cocaine (Ma *et al.* 2008a, Kiraly *et al.* 2013, Kiraly *et al.* 2010). In addition to the Kal7-mediated phenotypes, mice lacking all of the Kalirin isoforms ($KalSR^{KO}$) exhibit impaired neuromuscular and neuroendocrine function (Mandela *et al.* 2012, Mandela *et al.* 2014), decreased bone mass and diminished protection in a model of atherosclerosis (Wu *et al.* 2013, Huang *et al.* 2014).

Multiple promoter use adds further diversity to the protein products generated from the *Kalrn* gene (Mains *et al.* 2011, Johnson *et al.* 2000). Kalirin transcripts that include a Sec14 domain are generated from initiation sites in four promoters (A, B, C and D), each of which encodes a single, unique initial exon (Ex1A, 1B, 1C, 1D). The biophysical properties of the peptides encoded by these initial exons differ (Suppl. Table 1). The Ex1C peptide forms an amphipathic helix which interacts directly with phosphoinositide-containing liposomes (Miller *et al.* 2015); Ex1B encodes a negatively charged, unstructured peptide which does not interact with liposomes. While cSec14 (Sec14 domain preceded by Ex1C peptide) interacts with phosphoinositide-containing liposomes, bSec14 does not (Miller *et al.* 2015). Phosphoinositides play essential roles in mediating membrane/receptor trafficking, cytoskeletal organization and synaptogenesis (Ueda 2014, Rapoport *et al.* 2015).

We previously demonstrated a role for the Ex1C peptide in localizing cSec14 to the Golgi region in neuroendocrine cells (Miller *et al.* 2015), but its role in neurons has not been explored. Here, we identify striking developmental regulation of *Kalrn* promoter usage in rodent brain and use a mutant designed to reduce cSec14 domain interactions with the

charged head group of phosphoinositides to reveal functional consequences of promoter usage on Kalirin localization.

Materials and Methods

Experimental animals

Embryos from timed pregnant Sprague-Dawley rats (Charles River; gestational day 18) were used to make hippocampal and cortical cultures. C57BL/6 mice of both sexes (Jackson) were sacrificed to prepare brain tissue. All procedures were approved by our Institutional Animal Care and Use Committee and are consistent with ARRIVE guidelines (http://www.elsevier.com/__data/promis_misc/622936arrive_guidelines.pdf).

RNA extraction and polymerase chain reaction

RNA was prepared from cortex, hippocampus and striatum of individual male and female C57BL/6 mice using Trizol (Invitrogen) (Mains *et al.* 2011).

qRT-PCR—cDNA was prepared using iScript reverse transcriptase (BioRad) (Mains *et al.* 2011). Real-time PCR was performed with the following parameters: 95°C for 2 min, then 40X 95°C for 15 sec, 55°C for 15 sec, 68°C for 40 sec. Primer sequences and calculated melting temperatures are in Suppl. Table 2. The primer for mouse Exon1A was determined by BLAT search (http://genome.ucsc.edu/) against the mouse genome (GRCm38/mm10) using the rat U88157 sequence (nt 34456907-34456881), which places Ex1A 65kb upstream of Ex2 in mouse, as in rat and human (McPherson *et al.* 2004). All products were 120±5 nt by gel analysis, and maximum amplification/cycle for each primer set was 1.85–2.0. Data were analyzed using the relative cycle threshold (ΔCt) method with respect to GAPDH. Results are average exponentiated ΔCt values from 3–4 biological replicates/group ± SEM.

Long-range PCR—cDNA was prepared using Superscript III reverse transcriptase (Invitrogen) and Oligo-dT primers (Qiagen). PCR used the Expand Long Template PCR system (Roche) with 1.75 mM $MgCl_2$: 92°C for 2 min; [61°C for 30 sec; 68°C for 15 min; 92°C for 10 sec] × 10; [65°C for 30 sec; 68°C for 15 min; 92°C for 15 sec] × 40. Primers are listed in Suppl. Table 2.

Antibodies

Rabbit antibody (CT38) to the Kal-C-Helix peptide was generated at Covance Research Products (Hazleton, PA); 2 mg peptide (MTDRFWDQWYLWYLR) was linked to 4 mg keyhole limpet hemocyanin using 0.3% glutaraldehyde. Rabbits were immunized (0.3 mg conjugated peptide) and boosted at ~3 week intervals (0.1 mg conjugated peptide). Affinity-purification was performed using 4 mg peptide linked to 2 ml Affi-Gel 10 (BioRad). Antibodies used for Western blotting: affinity-purified rabbit polyclonal to Kalirin spectrin repeats 4 to 7 (Kal-SR4-7) (JH2581) (Penzes *et al.* 2000), affinity-purified rabbit polyclonal to Kal-Sec14 (CT302) (Yan *et al.* 2014), affinity-purified rabbit polyclonal to Kal-C-helix (CT38), rabbit polyclonal to C-terminus of Kal7 (JH2959) (Yan *et al.* 2014), mouse monoclonals to PSD95 (clone K28/43; NeuroMab Facility, University of California, Davis, CA), GAPDH (clone 6C5, MAB374; Millipore), Myc epitope tag [9E10 (Borjigin &

Nathans 1994)], NR2B (clone 59/20; NeuroMab Facility), GM130 (#610822; BD Transduction Laboratories), and calreticulin (#612136; BD Transduction Laboratories),

Primary antibodies used for immunostaining included rat anti-GFP (NacalaiTesque, Kyoto, Japan), mouse monoclonal to PSD95 (clone 28/43, 1:300; NeuroMab), and guinea pig antibody to Vglut1 (AB5909; Millipore). Primary antibodies were visualized with appropriate secondary antibodies: Cy3-donkey anti-mouse and fluorescein isothiocyanate (FITC)-donkey anti-rat immunoglobulin G (IgG) were from Jackson ImmunoResearch Laboratories (West Grove, PA); Alexa Fluor 633-goat anti-guinea pig and –goat anti-mouse IgG were from Molecular Probes (Eugene, OR).

Subcellular fractionation

Adult mouse forebrain homogenized in 10 volumes isotonic buffer with protease and phosphatase inhibitors was fractionated (Kiraly *et al.* 2011b). After separating the crude synaptosomal pellet, the supernatant was centrifuged to yield a membrane pellet (P3) and cytosol. LSM (lysed synaptosomal membranes) were fractionated by sucrose gradient to yield PSD's.

Immunoprecipitation and Western blot analysis

Samples were denatured with SDS and immunoprecipitated (Kiraly *et al.* 2011b); a 10-fold weight excess (NP-40/SDS) was added before antibody was added. Cytosol, P3, LSM and PSD fractions (500 μg protein; 250 μg for PSD) were tumbled overnight at 4°C with affinity-purified Kal-SR4-7 antibody or affinity-purified Kal-Sec14 antibody. Insoluble material was removed and supernatants were transferred to microfuge tubes containing 10 μl Protein A beads. After tumbling (1 h), unbound proteins were removed, resin was washed and bound proteins were eluted by boiling into SDS sample buffer. On a single gel, a large and a small percentage of each immunoprecipitate and a corresponding amount of recombinant cKal7 (transiently expressed in HEK-293 cells) was fractionated; after transfer to PVDF membranes, antibody CT38 was used to visualize the larger amount of sample and calibrator and antibody CT302 to visualize the smaller amount.

Rac1 biosensor and Rac activation assay

A FRET biosensor for activated Rac1 (Yan *et al.* 2016, Kedziora *et al.* 2016, Timmerman *et al.* 2015) was used to evaluate Rac1 activation in cells expressing Kal7 variants. FRET ratios were obtained using excitation at 420 nm and recording emission spectra from 440 to 600 nm. Protein expression levels were determined by Western blot analysis using antibodies to Kal7 (JH2959) and the biosensor Myc-tag. The FRET ratio (525/475) for each condition was plotted against the amount of Kal7 DNA used for transfection or against the observed protein expression level; similar answers were obtained using both approaches.

Primary neuronal cultures and transfection

Primary rat hippocampal neuron cultures were prepared from E18 Sprague–Dawley rats (Ma *et al.* 2008b, Ma *et al.* 2014, Gaier *et al.* 2013). For immunostaining, dissociated neurons were plated at 3×10^5 cells/1.75 cm^2 onto poly-L-lysine-coated coverslips. For expression of farnesylated-GFP [fGFP; (Francone *et al.* 2010)] neurons were nucleofected at plating

using program O-003 (Amaxa, Cologne, Germany) (Yan *et al.* 2014). For analysis of Sec14-EGFP and Kal7-EGFP expression in young neurons, cultures were transfected using Lipofectamine 2000 [0.7 μl transfection reagent (Life Technologies) per μg DNA] on *in vitro* day 3 (DIV3) and fixed 15 to 16 h later. For analysis of expression in more mature neurons, cultures transfected in the same way were fixed on DIV16.

Expression vectors

The pEAK vector (Ma *et al.* 2014) was used to express rat aKal7, bKal7, and cKal7; all previous exogenous expression studies utilized rat MycHis-aKal7 (Penzes *et al.* 2000, Penzes *et al.* 2001a, Yan *et al.* 2014, Ma *et al.* 2008a, Ma *et al.* 2014). To facilitate construction of expression vectors encoding bKal7(Spec9-EGFP) and cKal7(Spec9-EGFP), a silent *Nru1* mutation was inserted at nt93 of aKal7(Spec9-EGFP); insertion of non-dimerizing EGFP(A206K) (Sobota *et al.* 2006) into an exposed loop in spectrin repeat 9 was without effect on its ability to increase spine formation (Ma *et al.* 2014). The cSec14-EGFP and cKal7-EGFP vectors were mutagenized to express R15Q variants (Miller *et al.* 2015). All constructs were verified by DNA sequencing.

Immunocytochemistry and imaging

Neuronal cultures were fixed in 4% paraformaldehyde in PBS, permeabilized with 0.075% Triton X-100, blocked with 2 mg/ml BSA and doubly or triply stained with primary antibodies overnight at 4°C. All images were obtained using a Zeiss (Jena, Germany) Axiovert 200M microscope with a 63X oil objective and AxioVision software (Carl Zeiss Microscopy, LLC, Thornwood, NY, USA). Optical sectioning was achieved with the Zeiss ApoTome module; individual sections or multiple sections (three, taken at 0.4 μm intervals and compressed) were used as indicated.

Image analysis

Spine density and synaptic clusters were analyzed using MetaMorph image analysis software, (Molecular Devices, Sunnyvale, CA) (Ma *et al.* 2008b, Ma *et al.* 2014). Briefly, representative dendritic segments within 150 μm of the cell soma were measured and spines/synaptic clusters were counted manually. A line was drawn from the dendritic shaft to the tip of the spine head to measure spine length; dendritic protrusions less than 5 μm long were counted as dendritic spines. Postsynaptic cluster area was determined by manually tracing GFP-positive puncta. Length and area measurements were calibrated using a representative scale bar and data from each image (1 neuron/image) were averaged. All images were coded, then scored by a blinded observer. Decoded data were compared across groups and are presented as averages ± SEM.

Homology modeling and molecular docking

Homology modeling of cSec14 (residues 1–180; NCBI ID: AF230644) used the PHYRE 2 protein structure prediction server (Kelley *et al.* 2015). The cSec14 sequence underwent secondary structure prediction; the output was aligned and scored against the PHYRE database to produce a cSec14 domain tertiary homology model ensemble. From this ensemble, the top scoring PHYRE homology model was used as a representative cSec14

domain structure. For molecular docking, the three-dimensional coordinates of phosphatidylinositol 4-phosphate (PI(4)P) were adapted from the OSH6P-PI(4)P complex (PDB ID: 4PH7) and modeled as the 18:0/18:1 molecular species. The PDBQT format files of both PI(4)P and cSec14 were generated using the AutoDock Tools package provided by AutoDock Vina (Trott & Olson 2010). The PI(4)P molecule was docked as an independent rigid-body unit and the entire surface of the homology model was searched for possible binding pockets without bias.

Statistics

Statistical tests were performed using OpenOffice 4.0, Sigma Plot 11.0 or GraphPad Prism 7.0: T-Test, RM-ANOVA, whisker plots. Kolmogorov-Smirnov statistics were from Conover (Conover 1999).

Results

Kalrn promoter usage is developmentally regulated

Expression of transcripts encoding Kalirin isoforms with a Sec14 domain is initiated at one of four alternate promoters; the resulting transcripts include an initial exon (Ex1A, 1B, 1C, 1D) encoding a short peptide that precedes the common lipid-binding Sec14 domain (Fig.1A and B). To evaluate the physiological significance of *Kalrn* promoter usage in the nervous system, we used qPCR to assess transcript levels in mouse cortex, hippocampus and striatum from P1 through P60. Cortical and hippocampal RNA was also collected from E16 mice. Unique primers for each initial exon were paired with a common reverse primer in exon 3 (Fig.1B, Suppl. Table 2). Transcript levels with respect to GAPDH are shown in Fig.1C. In each brain region, we found that *Kalrn* promoter usage was developmentally regulated. Ex1B (Fig.1C, dashed blue lines) was highly expressed at early developmental time points, accounting for virtually 100% of embryonic *Kalrn* transcripts in cortex and hippocampus. Ex1C (Fig.1C, orange lines) expression was not detectable embryonically, but increased postnatally in all three regions. Interestingly, a developmental switch from use of Ex1B to Ex1C was observed between P1 and P21 in the hippocampus, with Ex1C comprising nearly 75% of the *Kalrn* transcripts in this tissue from P21 to P28; at P60, usage of Ex1B and Ex1C was equivalent. In contrast, in cortex, use of Ex1B was predominant throughout development. Ex1B and Ex1C transcript levels in the striatum were equivalent after P8. Notably, striatal expression of Ex1C was higher at P1 than in hippocampus and cortex, potentially reflecting earlier synaptogenesis in the striatum (Peixoto *et al.* 2016). Remarkably, although PCR products of the correct size were detected for all four primer sets, neither promoter A nor D was used appreciably in these brain regions at any time in development.

In order to determine whether the transcripts initiated at these two promoters accounted for most of the *Kalrn* transcripts, we analyzed the same samples using a primer set in Exon 10 (spectrin repeat 5); when normalized to GAPDH, Exon 10 transcript levels were approximately equal to the sum of Ex1B plus Ex1C transcript levels for all ages in all three tissues (not shown).

cKal7 protein is enriched in synaptic membranes and the postsynaptic density

The peptides encoded by Ex1B and Ex1C are remarkably different (Fig.2A, Suppl. Table 1). Mouse Ex1B encodes a long, negatively charged, unstructured peptide (Miller *et al.* 2015). Human *KALRN* Ex1B encodes the identical peptide and homologous peptides occur in other mammals and lower vertebrates. The Ex1C-peptide, which is identical in over 100 mammalian species, forms an amphipathic helix, with its hydrophobic and charged residues aligning on opposite sides of the helix. The amphipathic C-helix interacts with phosphoinositides and is essential for cKalSec14-mediated membrane interactions in neuroendocrine cells (Miller *et al.* 2015). Interestingly, despite the presence of a *Kalrn* gene, no Ex1C homolog was identified in lower animals, suggesting a specific role for this region in more evolved nervous systems. Notably, neither the invertebrate homologs of *Kalrn* (*dTrio* and *Unc-73*) nor *Trio*, a mammalian paralog of *Kalrn,* encode peptides that correspond to any of the Kalirin Ex1-peptides. Sequence homology between Kalirin and Trio is first apparent at the start of the Sec14 domain.

A previous study used long-range PCR to demonstrate that rat brain *Kalrn* transcripts that include Ex1B or Ex1C can terminate with 3′-exons unique to Kal7, Kal9 or Kal12 (Johnson *et al.* 2000). Using a similar PCR strategy to examine mouse cortical cDNA, we found the same answer (data not shown). Since these experiments do not provide an accurate comparison of Ex1B vs. Ex1C transcript levels, we sought an approach that could distinguish Kalirin proteins with the c-front from Kalirin proteins with the b-front; bKal7 (190,607 daltons) and cKal7 (191,196 daltons) differ by less than 600 daltons, precluding their separation by SDS-PAGE. Therefore, we developed an antibody to the Ex1C-peptide (Fig.2A). Affinity-purified Ex1C-peptide antibody recognized cKal7 and showed no cross-reactivity with bKal7 (Fig.2B). This signal was blocked by an excess of the immunogenic peptide (not shown). Attempts to develop an antibody to the Ex1B-peptide were not successful.

To evaluate *in vivo* cKal expression and subcellular localization, we performed a series of immunoprecipitation experiments following subcellular fractionation of adult mouse forebrain lysates. The success of the subcellular fractionation protocol was verified using antisera to NR2B and PSD95 (PSD markers), GM130 (Golgi marker), calreticulin (endoplasmic reticulum marker) and GAPDH (cytosol marker) (Fig.2C). GM130 and calreticulin were enriched in the P3 fraction, while GAPDH was enriched in cytosol and lysed synaptosomal cytosol (LSC). As expected, Kal7 was enriched in the lysed synaptosomal membrane (LSM) and postsynaptic density (PSD) fractions, along with NR2B, a subunit of the NMDA receptor, and PSD95, a major post-synaptic density scaffolding protein.

Total Kalirin was immunoprecipitated from cytosol, P3, LSM and PSD fractions from adult male and female mouse forebrain using a spectrin repeat region antibody (JH2581, Fig.2A). Immunoprecipitates were separated by SDS-PAGE and probed with Sec14 antibody (CT302) or Ex1C-peptide antibody (CT38, Fig.2A). Aliquots of recombinant cKal7 were included on each gel to enable quantification. To accommodate the diminished sensitivity of the Ex1C-peptide antibody, increased amounts of each immunoprecipitate and recombinant cKal7 were used for this antibody. As expected, cross-reactive proteins the size of Kal7,

Kal9 and Kal12 were detected in varying amounts in all four fractions using the Sec14 antibody (Fig.2D, right). When larger amounts of the same samples (fractionated on the same gel and transferred at the same time) were probed with the Ex1C-peptide antibody, the only band observed was the size of Kal7, even with longer exposures (Fig.2D, left). cKal7 was detected in the ER/Golgi (P3), LSM and PSD fractions, but not in the cytosol (Fig.2D).

To quantify the fraction of the total Kal7 accounted for by cKal7 in each fraction, recombinant cKal7 analyzed at the same time was used as a calibrator. The ratio of the Ex1C signal to the Sec14 signal for the calibrator sample established the ratio expected for samples containing only the c-front. The Ex1C to Sec14 ratio for Kal7 was essentially zero in the cytosol fraction (1.8±2.9%, n=5, SD) and was highest in the LSM and PSD fractions (Fig.2E); 36±4% (n=5, SD) of the Kal7 in the LSM fraction and 28±9% (n=5, SD) of the Kal7 in the PSD fraction was cKal7. In contrast, only 12±6% (n=5, SD) of the Kal7 in the P3 fraction was cKal7. Our finding that a third of the Kal7 in adult forebrain synaptosomal membranes had the c-front was consistent with our qPCR data from adult cortex (Fig.1C). These experiments demonstrate that the presence of the Kal-C-helix is sufficient to alter the subcellular localization of endogenous Kal7 in neurons.

Despite the fact that our long-range PCR data showed C-promoter usage in Kal9/12 transcripts, we were unable to detect any cKal9 or cKal12 protein using the Ex1C-peptide antibody (Fig.2D). Even with a much longer exposure of the Ex1C blot (Fig.2D, bottom) it was impossible to detect a band of cKal9 or cKal12 in any subcellular fraction. Quantification of the Ex1C/Sec14 signal ratio for Kal9 and Kal12 in the P3, LSM and PSD fraction indicated that the c-front accounted for no more than 3% of either isoform.

Endogenous cKal7 localizes to dendritic spines

We next used the affinity-purified Ex1C-peptide antibody to visualize cKal localization in cultured neurons using immunocytochemistry; based on our above analysis of Kal9 and Kal12, signal from the Ex1C-peptide antibody represents cKal7 (Fig.3). Rat hippocampal neurons were transfected at plating with a farnesylated-GFP construct (fEGFP), targeting EGFP to the plasma membrane (Francone *et al.* 2010) and facilitating dendritic spine visualization. After 22 DIV, neurons were fixed and stained with antibodies to Ex1C-peptide (red), vesicular glutamate transporter 1 (Vglut1, blue), and GFP (green). Ex1C-peptide signal was present in puncta localized to the tips of dendritic spines, closely juxtaposed to Vglut1 puncta, a marker of presynaptic terminals (Fig.3, yellow arrowheads); staining was blocked with synthetic-Ex1C peptide (not shown). Ex1C-peptide staining was also observed in the soma (Fig.3, white arrowheads in merged image).

Alternate promoter usage affects protein localization, not GEF activity

We used a Rac1 biosensor in a cell-based Rac1 activation assay to compare the GEF activity of bKal7 and cKal7 (Fig.4A). We compared the activity of these isoforms to the activity of aKal7, the only isoform used previously in exogenous expression systems. HEK cells were transfected with vector encoding the Dora-Rac1 biosensor and varying amounts of vector encoding each Kal7 isoform; carrier DNA was used to keep the total amount of DNA constant. For all constructs, we observed an increase in Rac1 activation with increasing

amounts of Kal7 DNA (Fig.4A and B). Equal amounts of aKal7, bKal7 and cKal7 vector produced the same FRET ratios (Fig.4B) and equivalent levels of protein expression (Fig. 4C).

We next asked whether the distinctly different subcellular localization of endogenous bKal7 and cKal7 could be recapitulated by expression of bKal7-EGFP and cKal7-EGFP. On DIV3, we transfected primary rat hippocampal neurons with vectors encoding EGFP, bKal7-EGFP, cKal7-EGFP or both bKal7-EGFP and cKal7-mCherry; protein localization was visualized on DIV4. bKal7-EGFP was distributed throughout the cell soma and in the processes; some punctate staining was observed in the soma and processes, although its intensity varied in different cells (Fig.4E; Suppl.Fig.1). In contrast, most of the cKal7-EGFP was present in punctate structures which were excluded from the nucleus and extended into the processes (Fig.4F; Suppl.Fig.2). Simultaneous expression of bKal7-EGFP and cKal7-mCherry confirmed these differences; while bKal7-EGFP extended into the neurites and could be seen in lamellipodia (green arrows) extending from the cell soma (Fig.4G; Suppl.Fig.3), cKal7-mCherry concentrated in puncta. Both isoforms frequently co-localized to the same punctate structures. This result is in agreement with our subcellular fractionation data demonstrating that bKal7 predominated in soluble fractions while both isoforms localized to particulate fractions. While not differing from bKal7 in its ability to activate Rac1, the increased association of cKal7 with membranes could alter its function at the PSD.

bKal7 and cKal7 form postsynaptic puncta that differ in size

Our qPCR data indicated that cKal7 expression began with synaptogenesis in all three brain regions evaluated. Additionally, we previously showed that removal of the Sec14 domain from Kal7 resulted in decreased spine length (Ma *et al.* 2014). To determine if promoter usage affected the ability of Kal7 to promote synaptogenesis, we expressed exogenous bKal7-EGFP or cKal7-EGFP in rat hippocampal neurons and evaluated dendritic protrusions at DIV15, when endogenous cKal7 expression has just begun to increase. Consistent with our biochemical experiments (Fig.2), both proteins co-localized extensively with PSD95 (Fig.5A); over 95% of the bKal7-EGFP and cKal7-EGFP puncta were coincident with PSD95 puncta. The bKal7-EGFP and cKal7-EGFP puncta were juxtaposed to Vglut1-positive presynaptic endings (Fig.5B), as expected based on the presence of both bKal7 and cKal7 in purified PSDs.

In order to determine whether bKal7-EGFP and cKal7-EGFP differed in their ability to localize to immature spines, GFP signal intensity was quantified. We first established a spine/dendrite intensity ratio to evaluate spine enrichment. Intensity ratios for bKal7-EGFP and cKal7-EGFP did not differ, but both were significantly higher than for EGFP, demonstrating enrichment of bKal7 and cKal7 in spines (Fig.6A). The linear density of GFP-positive puncta along the dendrites was also similar in bKal7-EGFP and cKal7-EGFP-expressing neurons; both isoforms of Kal7 caused a robust increase in the linear density of postsynaptic puncta compared with the EGFP control (Fig.6B). Similar increases were shown following expression of exogenous myc-tagged aKal7 (myc-aKal7) (Ma *et al.* 2008b, Ma *et al.* 2014). We observed no difference across groups in the number of GFP-positive puncta apposed to Vglut1-positive puncta (Fig.6C), indicating that bKal7-EGFP and cKal7-

EGFP expressing neurons were equally capable of attracting excitatory presynaptic endings. In addition to spine density, the size and shape of synaptic contacts bears functional significance. Interestingly, by quantifying EGFP-puncta area, we found that cKal7-EGFP puncta were significantly smaller than bKal7-EGFP puncta (Fig.6D). Our exogenous expression data suggest that endogenous cKal7, which is produced only when *Kalrn* promoter C usage is switched on during development, forms postsynaptic puncta that are smaller than the puncta formed by bKal7.

Mutation of predicted phosphoinositide head group binding site in Ex1C alters cSec14 and cKal7 localization

A major role of Kal7 is coordinating the cytoskeletal dynamics underlying structural growth, maintenance and plasticity in dendritic spines. Although attention has focused on GEF domain activation of Rac1 and RhoG, phosphoinositides are also key regulators of cytoskeletal dynamics (Ueda 2014, Hille *et al.* 2014, Rapoport *et al.* 2015). Previous studies demonstrated that the Ex1C amphipathic helix plays an essential role in the interaction of the cSec14 domain of Kalirin with phosphoinositides (Miller *et al.* 2015). To explore the possibility that phosphoinositide binding to cSec14 contributes to Kal7 function, we used the PHYRE 2 server (Kelley *et al.* 2015) to generate a cSec14 homology model. Not surprisingly, the highest confidence model (98% of residues modeled at >90% confidence) was based on the crystal structure of *Saccharomyces cerevisiae* Sec14 family homology 3 (Sfh3) (PDB ID: 4FMM). In this model, Kalirin cSec14 adopts a compact, globular α/β mixed fold featuring a large hydrophobic pocket bordered by five antiparallel β-strands and two long α-helices, unequivocally reminiscent of the core Sec14 fold (Fig.7A). The PI(4)P molecule was then docked as a rigid body unit to the cSec14 model using AutoDock Vina (Trott & Olson 2010). In most of the lowest binding energy docked conformations, PI(4)P bound in the hydrophobic pocket, with the inositol head group coordinated near the protein surface and the acyl chains buried in the cavity.

Two of the Arg residues expected to reside on the hydrophilic surface of the KalC-helix (Arg^{15} and Arg^{18}) were predicted to interact with the phosphorylated inositol, forming a lid that locks the lipid in place. Since the other residues predicted to interact with the bound phosphoinositide were shared with bSec14, we wondered if simply mutating Arg^{15} to Gln would alter the behavior of cSec14-EGFP. We used transient expression in young neurons to distinguish the behavior of cSec14-EGFP from that of bSec14-EGFP and to evaluate the effect of the R15Q mutation. bSec14-EGFP was uniformly distributed throughout the soma and initial processes (Fig.7B; Suppl.Fig.4A). In contrast, cSec14-EGFP was present in puncta excluded from the nucleus (Fig.7C; Suppl.Fig.4B); although found near the Golgi complex (GM130), cSec14-EGFP puncta were often distinct from this structure. At this stage of development, GM130 positive Golgi outposts were not detected in neurites. R15Q-cSec14-EGFP (Fig.7D; Suppl.Fig.4C,D) was localized in a manner more closely resembling bSec14-EGFP than cSec14-EGFP (Fig. 7B,E), with very few puncta observed in neurites.

We next asked whether introduction of the same mutation into cKal7 (R15Q-cKal7-EGFP) affected its localization. cKal7-mCherry and R15Q-cKal7-EGFP were co-expressed (Fig.7F; Suppl.Fig.4D); while cKal7 and R15Q-cKal7 overlapped extensively, expression of R15Q-

cKal7 was more diffuse (like bKal7) with variable ratios of the two fluorophores in different puncta. Over half of the neurons expressing cKal7-EGFP had lamellipodia extending from their soma and neurites; the prevalence of lamellipodia was significantly reduced in neurons expressing R15Q-cKal7-EGFP (Fig.7G). These data argue that the phospholipid-binding pocket in cSec14 is one determinant of cKal7 localization in young neurons and its effect on cell morphology.

Discussion

Alternate promoters

Use of multiple promoters serves as a major source of genetic and proteomic diversity, rivaling that of alternative splicing (Landry *et al.* 2003, Shabalina *et al.* 2014). Recent estimates suggest that nearly half of all protein-coding genes in the human genome have multiple promoters (Kimura *et al.* 2006, Davuluri *et al.* 2008), many of which are conserved in mouse (Baek *et al.* 2007). We demonstrated that alternate promoters add to the diversity of *Kalrn* transcripts in a developmentally-regulated, region-specific and functionally significant manner. For some genes, differential promoter usage results in alternate 5′ untranslated regions, with no change in the protein. Other genes utilize alternate promoters in a manner similar to *Kalrn*. The protocadherin (*Pcdh*) genes, which encode a family of cell surface proteins expressed in the brain, each have more than a dozen alternative initiation exons, which splice to a common C-terminus (Tasic *et al.* 2002). Interestingly, *Pcdh* promoter choice affects 3′-alternative splicing of the gene as well, and isoforms are differentially expressed in different cell types (Tasic *et al.* 2002, Brown *et al.* 2014, Lamas-Macieras *et al.* 2016).

While mRNA transcripts encoding cKal7 and cKal9 or cKal12 were detected, we were unable to detect cKal9 or cKal12 protein. Several factors may contribute to this observation. Coordinated changes in the splicing events that lead to use of the *Kalrn* C-Promoter and the single exon unique to Kal7 could make transcripts encoding cKal9 and cKal12 scarce. Decreased translatability of transcripts encoding cKal9 and cKal12 vs. cKal7 or decreased stability of cKal9 and cKal12 vs. cKal7 protein could account for the observed difference.

Given the prevalence of alternate promoters in the human genome, it is not surprising that aberrant promoter usage has been associated with many disease conditions (Landry *et al.* 2003, Davuluri *et al.* 2008), suggesting that genes with alternate promoters are more likely to be associated with disease (Davuluri *et al.* 2008, Liu 2010). Brain derived neurotrophic factor (BDNF) utilizes multiple promoters in a tissue-specific manner, and promoter usage is altered after kainite-induced seizures (Timmusk *et al.* 1993). A single nucleotide polymorphism (SNP) in the promoter region of the 5-HT2A serotonin receptor affects promoter activity and is associated with psychiatric disorders (Parsons *et al.* 2004). Interestingly, genetic linkage studies have identified several SNPs within the promoter region of *KALRN*. Two SNPs, one just upstream of Ex1B (rs12637456) and another midway between Ex1B and Ex1C (rs9289231), are associated with coronary artery disease (Boroumand *et al.* 2014, Wang *et al.* 2007, Horne *et al.* 2009). Three SNPs, one just upstream of exon 2 (rs17286604) and two located just after exon 3 (rs11712039; rs11712619), are risk factors for ischemic stroke (Krug *et al.* 2010, Ikram *et al.* 2009).

There are marked similarities across mammalian species in the 2 kb region immediately upstream of *KALRN* Ex1B and in the 2 kb region upstream of *KALRN* Ex1C; 50–200 nt motifs, which could form binding sites for regulatory factors, are highly conserved (McPherson *et al.* 2004). Consistent with the observed difference in *Kalrn* Ex1B vs. Ex1C usage during rodent development, the two promoter regions share almost no sequence homology. *Kalrn* Ex1C usage is turned on at the same time as many other genes essential for synapse formation; it will be interesting to identify any common factors involved in initiating expression of these genes. There are few genes in which the distance between the initial and second exon is as large as it is in *KALRN* (Fig.1B). *TRIO*, a Kalirin paralog, shares this unusual feature with *KALRN*; the initial *TRIO* exon is located 127 kb upstream of its second exon (NM_007118.2).

Identification of two sub-populations of Kal7

bKal7 and cKal7 differ only in their N-terminal ~25 amino acids, yet our data indicate substantial functional differences. Biochemical and histological experiments revealed that both bKal7 and cKal7 localized to dendritic spines, suggesting the presence of two sub-populations of Kal7 within this compartment. This notion is consistent with results from a study utilizing serial section electron microscopy and immunogold labeling to visualize Kal7 within dendritic spines (Nicholson *et al.* 2012). Kal7 was identified in both synaptic (closely associated with the PSD) and extrasynaptic microdomains, which differentially contribute to PSD size and spine volume. The number of extrasynaptic Kal7 particles was strongly correlated with increased PSD area and increased spine volume; in contrast, synaptically-localized Kal7 was only weakly correlated to these measures. Both bKal7 and cKal7 were localized to the PSD; the absence of cKal7 from the cytosol indicates that soluble Kal7 is largely bKal7. The dynamic actin pools underlying structural plasticity are mostly extrasynaptic (Frost *et al.* 2010, Honkura *et al.* 2008), suggesting that bKal7 may be more suited to affecting cytoskeletal dynamics within spines. Indeed, our data show that bKal7-EGFP forms larger synaptic EGFP-puncta than cKal7-EGFP when exogenously expressed, despite the fact that the isoforms do not differ in their GEF activity. Immunogold labeling will be required to explore cKal7 localization further; a more potent Ex1C-specific antibody will be essential for this type of study.

Notably, until now, every study employing exogenous expression of Kalirin has utilized aKal7, the first isoform cloned; however, our qPCR data demonstrate that promoter A is rarely used in rodent brain. Given the clear promoter-specific effects on Kal7 localization and function, a switch to expression of Kalirin transcripts that include Ex1B and/or Ex1C is essential. Our attempts to achieve isoform-specific knockdown of bKal7 and cKal7 expression have not yet been successful; shRNAs targeting the limited region specific to each mRNA were ineffective. The fact that Ex1C occurs only in mammals, is highly conserved and expressed when synaptogenesis occurs suggests that it plays an important role in coordinating synaptic structure and function.

A link between *Kalrn*, phosphoinositides and actin dynamics at the synapse

In addition to cytoskeletal demands, the expression of structural and functional synaptic plasticity requires on-demand trafficking of membrane proteins and lipids to and from the

surface (Park *et al.* 2006, Park *et al.* 2004), a process requiring actin. Despite this fact, the mechanisms by which actin dynamics and membrane trafficking are coordinated within spines remain enigmatic. Phosphoinositides, which bind to Kalirin cSec14 but not to Kalirin bSec14 (Miller *et al.* 2015), play crucial roles in membrane trafficking throughout the cell and at the synapse (Wenk & De Camilli 2004, Di Paolo & De Camilli 2006, Waugh 2015). For example, NMDA receptor stimulation causes phosphatidylinositol (3,4,5)trisphosphate (PIP_3) accumulation in the plasma membrane where it aids in AMPA receptor stabilization (Arendt *et al.* 2010, Arendt *et al.* 2014). The role of $PI(4,5)P_2$ in modulating ion channel function is well-documented (Hille *et al.* 2014), and metabolism of this lipid by the lipid phosphatase, synaptojanin 1, is required for proper AMPA receptor internalization (Gong & De Camilli 2008). Aberrant phosphoinositide metabolism is implicated in Autism and Down's Syndrome pathology (Murphy *et al.* 2000, Gupta *et al.* 2014, Voronov *et al.* 2008).

Our previous work established that Kal-Ex1C encodes an amphipathic helix which binds phosphoinositides and is essential for cSec14-mediated membrane interactions (Miller *et al.* 2015). In this study, we found that Ex1C expression was initiated around the time of synaptogenesis and maintained in adult mouse brain. bKal7 and cKal7 did not differ from aKal7 in their Rac1 GEF activity as assessed in HEK293 cells. Nevertheless, expression of EGFP-tagged bKal7 and cKal7 revealed differences in protein localization and function. Most strikingly, although colocalized with PSD95, the EGFP-positive puncta formed by cKal7-EGFP were smaller than those formed by bKal7-EGFP. As observed for Kalirin, the Sec14 domains of Dbs (Kostenko *et al.* 2005) and protoDbl (Ognibene *et al.* 2014), related Rho GEFs, affect protein localization and function without altering GEF activity. Differences in localization were especially pronounced following expression of the isolated Sec14 domains in DIV3 neurons, before the *Kalrn* promoter C is normally used; bSec14-EGFP was diffusely distributed while cSec14-EGFP was associated with puncta (Fig. 7B,C). Based on homology modeling, a single residue unique to Ex1C and located in the lid keeping PI(4)P in the hydrophobic pocket common to bSec14 and cSec14 was mutated (R15Q). Remarkably, introduction of this single mutation into cSec14-EGFP and into cKal7-EGFP altered their localization in transfected neurons. Local control of phosphoinositide levels in neurons expressing close to endogenous levels of Kal7 will be needed to understand the functional significance of promoter usage, but our combined data suggest that cKal7 plays a unique role in coordinating membrane and cytoskeletal dynamics at the PSD.

Supplementary Material

Refer to Web version on PubMed Central for supplementary material.

Acknowledgments

We thank Darlene D'Amato, Taylor LaRese and Yanping Wang for laboratory support and Andrew Yanik for quantifying multiple images. This work was supported by National Institutes of Health grants DK-032948 and GM-117061.

Abbreviations

Kal7	Kalirin 7

Kal9	Kalirin 9
Kal12	Kalirin 12
Kal-C-helix	helix encoded by the C-promoter
cKal	any isoform of Kalirin initiated from the *Kalrn* C-promoter
KalSR^{KO}	mice lacking all isoforms of Kalirin
Kal-SR4-7	spectrin repeats 4 to 7 of Kalirin
Kal7(Spec9-EGFP)	Kal7 with EGFP inserted into a loop in spectrin repeat 9
Rho-GEF	GDP/GTP exchange factor for Rho
PSD	post-synaptic density
fEGFP	farnesylated-EGFP
PI(4)P	phosphatidylinositol-4-phosphate
DIV	days *in vitro*
P2	crude synaptosomal pellet
P3	ER/Golgi enriched pellet
S3	cytosol
LSM	lysed synaptosomal membrane pellet
LSC	lysed synaptosomal cytosol

References

Arendt KL, Benoist M, Lario A, Draffin JE, Munoz M, Esteban JA. PTEN counteracts PIP3 upregulation in spines during NMDA-receptor-dependent long-term depression. J Cell Sci. 2014; 127:5253–5260. [PubMed: 25335889]

Arendt KL, Royo M, Fernandez-Monreal M, Knafo S, Petrok CN, Martens JR, Esteban JA. PIP3 controls synaptic function by maintaining AMPA receptor clustering at the postsynaptic membrane. Nat Neurosci. 2010; 13:36–44. [PubMed: 20010819]

Baek D, Davis C, Ewing B, Gordon D, Green P. Characterization and predictive discovery of evolutionarily conserved mammalian alternative promoters. Genome Res. 2007; 17:145–155. [PubMed: 17210929]

Borjigin J, Nathans J. Insertional mutagenesis as a probe of rhodopsin's topography, stability, and activity. J Biol Chem. 1994; 269:14715–14722. [PubMed: 7514180]

Boroumand M, Ziaee S, Zarghami N, Anvari MS, Cheraghi S, Abbasi SH, Jalali A, Pourgholi L. The Kalirin Gene rs9289231 Polymorphism as a Novel Predisposing Marker for Coronary Artery Disease. Laboratory medicine. 2014; 45:302–306. [PubMed: 25316661]

Brown JB, Boley N, Eisman R, May GE, Graveley BR, Celniker SE. Diversity and dynamics of the Drosophila transcriptome. Nature Biotechnol. 2014; 512:393–399.

Conover, WJ. Statistics of the Kolmogorov-Smirnov type. In: Conover, WJ., editor. Practical nonparametric statistics. John Wiley & Sons, Inc; New York: 1999. p. 428-473.

Davuluri RV, Suzuki Y, Sugano S, Plass C, Huang TH. The functional consequences of alternative promoter use in mammalian genomes. Trends Genet. 2008; 24:167–177. [PubMed: 18329129]

Di Paolo G, De Camilli P. Phosphoinositides in cell regulation and membrane dynamics. Nature. 2006; 443:651–657. [PubMed: 17035995]

Francone VP, Ifrim MF, Rajagopal C, Leddy CJ, Wang Y, Carson JH, Mains RE, Eipper BA. Signaling from the secretory granule to the nucleus: Uhmk1 and PAM. Mol Endocrinol. 2010; 24:1543–1558. [PubMed: 20573687]

Frost NA, Shroff H, Kong H, Betzig E, Blanpied TA. Single-molecule discrimination of discrete perisynaptic and distributed sites of actin filament assembly within dendritic spines. Neuron. 2010; 67:86–99. [PubMed: 20624594]

Gaier ED, Miller MB, Ralle M, Aryal D, Wetsel WC, Mains RE, Eipper BA. Peptidylglycine alpha-amidating monooxygenase heterozygosity alters brain copper handling with region specificity. J Neurochem. 2013; 127:605–619. [PubMed: 24032518]

Gong LW, De Camilli P. Regulation of postsynaptic AMPA responses by synaptojanin 1. Proc Natl Acad Sci U S A. 2008; 105:17561–17566. [PubMed: 18987319]

Gupta AR, Pirruccello M, Cheng F, et al. Rare deleterious mutations of the gene EFR3A in autism spectrum disorders. Molecular autism. 2014; 5:31. [PubMed: 24860643]

Hille B, Dickson EJ, Kruse M, Vivas O, Suh BC. Phosphoinositides regulate ion channels. Biochim Biophys Acta. 2014; 1851:844–856. [PubMed: 25241941]

Honkura N, Matsuzaki M, Noguchi J, Ellis-Davies GC, Kasai H. The subspine organization of actin fibers regulates the structure and plasticity of dendritic spines. Neuron. 2008; 57:719–729. [PubMed: 18341992]

Horne BD, Hauser ER, Wang L, Muhlestein JB, Anderson JL, Carlquist JF, Shah SH, Kraus WE. Validation study of genetic associations with coronary artery disease on chromosome 3q13-21 and potential effect modification by smoking. Ann Hum Genet. 2009; 73:551–558. [PubMed: 19706030]

Huang S, Eleniste PP, Wayakanon K, Mandela P, Eipper BA, Mains RE, Allen MR, Bruzzaniti A. The Rho-GEF Kalirin regulates bone mass and the function of osteoblasts and osteoclasts. Bone. 2014; 60:235–245. [PubMed: 24380811]

Ikram MA, Seshadri S, Bis JC, et al. Genomewide association studies of stroke. N Engl J Med. 2009; 360:1718–1728. [PubMed: 19369658]

Johnson RC, Penzes P, Eipper BA, Mains RE. Isoforms of kalirin, a neuronal Dbl family member, generated through use of different 5′- and 3′-ends along with an internal translational initiation site. J Biol Chem. 2000; 275:19324–19333. [PubMed: 10777487]

Kedziora KM, Leyton-Puig D, Argenzio E, et al. Rapid Remodeling of Invadosomes by Gi-coupled Receptors: Dissecting the role of Rho GTPases. J Biol Chem. 2016; 291:4323–4333. [PubMed: 26740622]

Kelley LA, Mezulis S, Yates CM, Wass MN, Sternberg MJ. The Phyre2 web portal for protein modeling, prediction and analysis. Nat Protoc. 2015; 10:845–858. [PubMed: 25950237]

Kimura K, Wakamatsu A, Suzuki Y, et al. Diversification of transcriptional modulation: large-scale identification and characterization of putative alternative promoters of human genes. Genome Res. 2006; 16:55–65. [PubMed: 16344560]

Kiraly DD, Lemtiri-Chlieh F, Levine ES, Mains RE, Eipper BA. Kalirin Binds the NR2B Subunit of the NMDA Receptor, Altering Its Synaptic Localization and Function. J Neurosci. 2011a; 31:12554–12565. [PubMed: 21880917]

Kiraly DD, Lemtiri-Chlieh F, Levine ES, Mains RE, Eipper BA. Kalirin binds the NR2B subunit of the NMDA receptor, altering its synaptic localization and function. J Neurosci. 2011b; 31:12554–12565. [PubMed: 21880917]

Kiraly DD, Ma XM, Mazzone CM, Xin X, Mains RE, Eipper BA. Behavioral and morphological responses to cocaine require kalirin7. Biol Psychiatry. 2010; 68:249–255. [PubMed: 20452575]

Kiraly DD, Nemirovsky NE, LaRese TP, Tomek SE, Yahn SL, Olive MF, Eipper BA, Mains RE. Constitutive knockout of kalirin-7 leads to increased rates of cocaine self-administration. Mol Pharmacol. 2013; 84:582–590. [PubMed: 23894151]

Kostenko EV, Mahon GM, Cheng L, Whitehead IP. The Sec14 Homology Domain Regulates the Cellular Distribution and Transforming Activity of the Rho-specific Guanine Nucleotide Exchange Factor Dbs. J Biol Chem. 2005; 280:2807–2817. [PubMed: 15531584]

Krug T, Manso H, Gouveia L, et al. Kalirin: a novel genetic risk factor for ischemic stroke. Hum Genet. 2010; 127:513–523. [PubMed: 20107840]

Lamas-Macieras M, Singh BN, Hampsey M, Freire-Picos MA. Promoter-Terminator Gene Loops Affect Alternative 3′-End Processing in Yeast. J Biol Chem. 2016; 291:8960–8968. [PubMed: 26929407]

Landry JR, Mager DL, Wilhelm BT. Complex controls: the role of alternative promoters in mammalian genomes. Trends Genet. 2003; 19:640–648. [PubMed: 14585616]

Lemtiri-Chlieh F, Zhao L, Kiraly DD, Eipper BA, Mains RE, Levine ES. Kalirin-7 is necessary for normal NMDA receptor-dependent synaptic plasticity. BMC Neurosci. 2011; 12:126. [PubMed: 22182308]

Liu S. Increasing alternative promoter repertories is positively associated with differential expression and disease susceptibility. PLoS One. 2010; 5:e9482. [PubMed: 20208995]

Lu J, Luo C, Bali KK, Xie RG, Mains RE, Eipper BA, Kuner R. A role for Kalirin-7 in nociceptive sensitization via activity-dependent modulation of spinal synapses. Nat Commun. 2015; 6:6820. [PubMed: 25865668]

Ma XM, Kiraly DD, Gaier ED, Wang Y, Kim EJ, Levine ES, Eipper BA, Mains RE. Kalirin-7 is required for synaptic structure and function. J Neurosci. 2008a; 28:12368–12382. [PubMed: 19020030]

Ma XM, Miller MB, Vishwanatha KS, Gross MJ, Wang Y, Abbott T, Lam TT, Mains RE, Eipper BA. Nonenzymatic domains of Kalirin7 contribute to spine morphogenesis through interactions with phosphoinositides and Abl. Mol Biol Cell. 2014; 25:1458–1471. [PubMed: 24600045]

Ma XM, Wang Y, Ferraro F, Mains RE, Eipper BA. Kalirin-7 is an essential component of both shaft and spine excitatory synapses in hippocampal interneurons. J Neurosci. 2008b; 28:711–724. [PubMed: 18199770]

Mains RE, Kiraly DD, Eipper-Mains JE, Ma XM, Eipper BA. Kalrn promoter usage and isoform expression respond to chronic cocaine exposure. BMC Neurosci. 2011; 12:20. [PubMed: 21329509]

Mandela P, Yan Y, LaRese T, Eipper BA, Mains RE. Elimination of Kalrn expression in POMC cells reduces anxiety-like behavior and contextual fear learning. Horm Behav. 2014; 66:430–438. [PubMed: 25014196]

Mandela P, Yankova M, Conti LH, Ma XM, Grady J, Eipper BA, Mains RE. Kalrn plays key roles within and outside of the nervous system. BMC Neurosci. 2012; 13:136. [PubMed: 23116210]

McPherson CE, Eipper BA, Mains RE. Kalirin Expression Is Regulated by Multiple Promoters. J Mol Neurosci. 2004; 22:51–62. [PubMed: 14742910]

Miller MB, Vishwanatha KS, Mains RE, Eipper BA. An N-terminal Amphipathic Helix Binds Phosphoinositides and Enhances Kalirin Sec14 Domain-mediated Membrane Interactions. J Biol Chem. 2015; 290:13541–13555. [PubMed: 25861993]

Murphy EJ, Schapiro MB, Rapoport SI, Shetty HU. Phospholipid composition and levels are altered in Down syndrome brain. Brain Res. 2000; 867:9–18. [PubMed: 10837793]

Nicholson DA, Cahill ME, Tulisiak CT, Geinisman Y, Penzes P. Spatially restricted actin-regulatory signaling contributes to synapse morphology. J Neurochem. 2012; 121:852–860. [PubMed: 22458534]

Ognibene M, Vanni C, Blengio F, Segalerba D, Varesio L, Eva A. Identification of a novel mouse Dbl proto-oncogene splice variant: Evidence that SEC14 domain is involved in GEF activity regulation. Gene. 2014; 537:220–229. [PubMed: 24412292]

Park M, Penick EC, Edwards JG, Kauer JA, Ehlers MD. Recycling endosomes supply AMPA receptors for LTP. Science. 2004; 305:1972–1975. [PubMed: 15448273]

Park M, Salgado JM, Ostroff L, Helton TD, Robinson CG, Harris KM, Ehlers MD. Plasticity-induced growth of dendritic spines by exocytic trafficking from recycling endosomes. Neuron. 2006; 52:817–830. [PubMed: 17145503]

Parsons MJ, D'Souza UM, Arranz MJ, Kerwin RW, Makoff AJ. The-1438A/G polymorphism in the 5-hydroxytryptamine type 2A receptor gene affects promoter activity. Biol Psychiatry. 2004; 56:406–410. [PubMed: 15364038]

Peixoto RT, Wang W, Croney DM, Kozorovitskiy Y, Sabatini BL. Early hyperactivity and precocious maturation of corticostriatal circuits in Shank3B−/−mice. Nat Neurosci. 2016; 19:716–724. [PubMed: 26928064]

Penzes P, Beeser A, Chernoff J, Schiller MR, Eipper BA, Mains RE, Huganir RL. Rapid induction of dendritic spine morphogenesis by trans-synaptic ephrinB-EphB receptor activation of the Rho-GEF kalirin. Neuron. 2003; 37:263–274. [PubMed: 12546821]

Penzes P, Johnson RC, Alam MR, Kambampati V, Mains RE, Eipper BA. An isoform of kalirin, a brain-specific GDP/GTP exchange factor, is enriched in the postsynaptic density fraction. J Biol Chem. 2000; 275:6395–6403. [PubMed: 10692441]

Penzes P, Johnson RC, Kambampati V, Mains RE, Eipper BA. Distinct roles for the two Rho GDP/GTP exchange factor domains of kalirin in regulation of neurite growth and neuronal morphology. J Neurosci. 2001a; 21:8426–8434. [PubMed: 11606631]

Penzes P, Johnson RC, Sattler R, Zhang X, Huganir RL, Kambampati V, Mains RE, Eipper BA. The neuronal Rho-GEF Kalirin-7 interacts with PDZ domain-containing proteins and regulates dendritic morphogenesis. Neuron. 2001b; 29:229–242. [PubMed: 11182094]

Rapoport SI, Primiani CT, Chen CT, Ahn K, Ryan VH. Coordinated Expression of Phosphoinositide Metabolic Genes during Development and Aging of Human Dorsolateral Prefrontal Cortex. PLoS One. 2015; 10:e0132675. [PubMed: 26168237]

Shabalina SA, Ogurtsov AY, Spiridonov NA, Koonin EV. Evolution at protein ends: major contribution of alternative transcription initiation and termination to the transcriptome and proteome diversity in mammals. Nucleic Acids Res. 2014; 42:7132–7144. [PubMed: 24792168]

Sobota JA, Ferraro F, Back N, Eipper BA, Mains RE. Not all secretory granules are created equal: Partitioning of soluble content proteins. Mol Biol Cell. 2006; 17:5038–5052. [PubMed: 17005911]

Tasic B, Nabholz CE, Baldwin KK, et al. Promoter choice determines splice site selection in protocadherin alpha and gamma pre-mRNA splicing. Mol Cell. 2002; 10:21–33. [PubMed: 12150904]

Timmerman I, Heemskerk N, Kroon J, Wu Y, Huveneers S, van Buul JD. A local VE-cadherin and Trio-based signaling complex stabilizes endothelial junctions through Rac1. J Cell Sci. 2015; 128:3041–3054. [PubMed: 26116572]

Timmusk T, Palm K, Metsis M, Reintam T, Paalme V, Saarma M, Persson H. Multiple promoters direct tissue-specific expression of the rat BDNF gene. Neuron. 1993; 10:475–489. [PubMed: 8461137]

Trott O, Olson AJ. AutoDock Vina: improving the speed and accuracy of docking with a new scoring function, efficient optimization, and multithreading. J Comput Chem. 2010; 31:455–461. [PubMed: 19499576]

Ueda Y. The Role of Phosphoinositides in Synapse Function. Mol Neurobiol. 2014; 50:821–838. [PubMed: 24935718]

Voronov SV, Frere SG, Giovedi S, et al. Synaptojanin 1-linked phosphoinositide dyshomeostasis and cognitive deficits in mouse models of Down's syndrome. Proc Natl Acad Sci U S A. 2008; 105:9415–9420. [PubMed: 18591654]

Wang L, Hauser ER, Shah SH, et al. Peakwide mapping on chromosome 3q13 identifies the kalirin gene as a novel candidate gene for coronary artery disease. Am J Hum Genet. 2007; 80:650–663. [PubMed: 17357071]

Waugh MG. PIPs in neurological diseases. Biochim Biophys Acta. 2015; 1851:1066–1082. [PubMed: 25680866]

Wenk MR, De Camilli P. Protein-lipid interactions and phosphoinositide metabolism in membrane traffic: insights from vesicle recycling in nerve terminals. Proc Natl Acad Sci U S A. 2004; 101:8262–8269. [PubMed: 15146067]

Wu JH, Fanaroff AC, Sharma KC, Smith LS, Brian L, Eipper BA, Mains RE, Freedman NJ, Zhang L. Kalirin promotes neointimal hyperplasia by activating Rac in smooth muscle cells. Arterioscler Thromb Vasc Biol. 2013; 33:702–708. [PubMed: 23288169]

Yan Y, Eipper BA, Mains RE. Kalirin-9 and Kalirin-12 Play Essential Roles in Dendritic Outgrowth and Branching. Cereb Cortex. 2015; 25:3487–3501. [PubMed: 25146373]

Yan Y, Eipper BA, Mains RE. Kalirin is required for BDNF-TrkB stimulated neurite outgrowth and branching. Neuropharmacology. 2016; 107:227–238. [PubMed: 27036892]

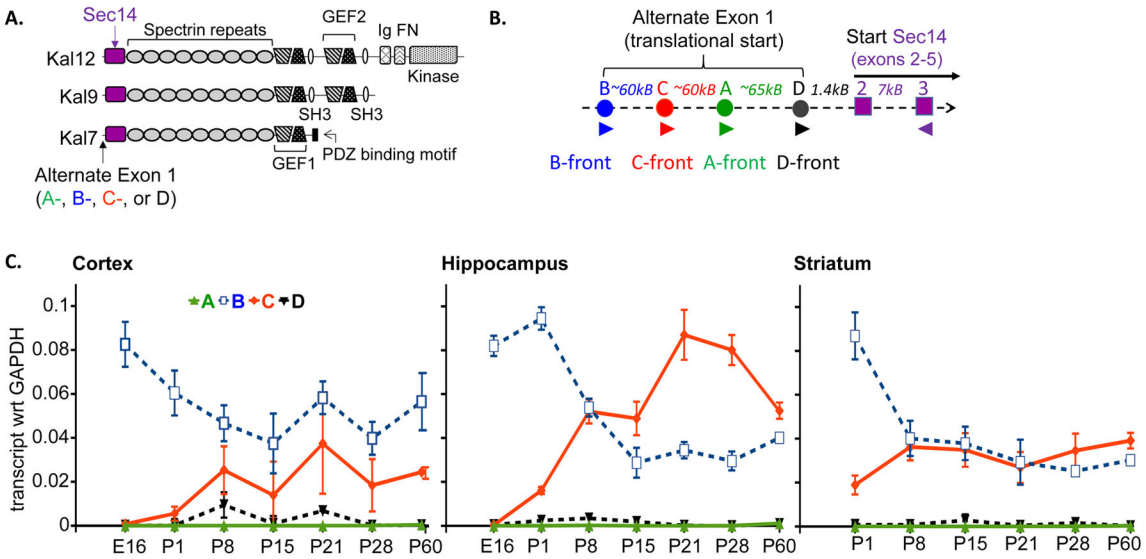

Figure 1. Full-length Kalirin splice variants and alternate promoters

A. Developmentally regulated, tissue-specific alternative splicing of *Kalrn* generates three major proteins, Kal12, Kal9 and Kal7; domains are indicated. **B.** Diagram of alternate promoters in the rat *Kalrn* gene. Promoters are separated by introns (57–65 kb) located 1.4–180 kb upstream of common exon 2; a similar arrangement occurs in mouse and human. Locations of qPCR primers used in Fig.1C are indicated (arrow heads). **C.** qPCR data showing *Kalrn* Exon 1 (Ex1) transcript levels in cortex (**left**), hippocampus (**middle**) and striatum (**right**) across development. Data are shown as group averages (ΔCt with respect to GAPDH [exponentiated]) ± SEM; n = 3–4 animals per time point.

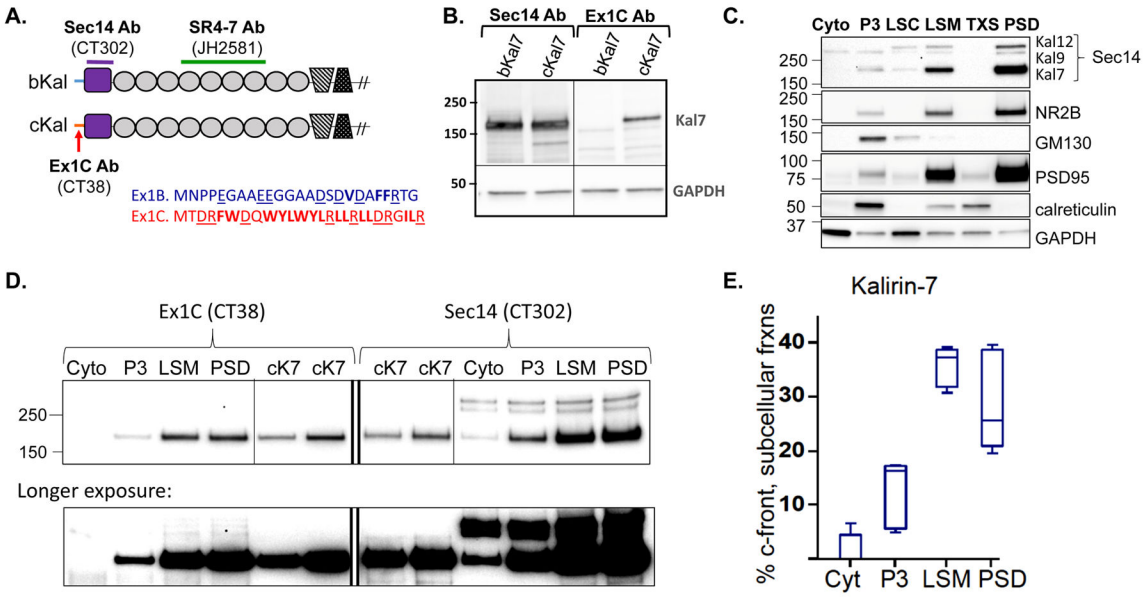

Figure 2. Subcellular localization of cKal7

A. Diagram illustrating epitopes recognized by antibodies used for immunoprecipitation: the Kal-SR4-7 and Sec14 antibodies recognize isoforms generated from the A-, B- and C-promoters equally; the Ex1C-peptide antibody only recognizes isoforms generated from the C-promoter (**B**). Ex1 peptide sequences are shown, with charged residues underlined and hydrophobic residues in boldface. **B.** Western blot of lysates from HEK cells expressing bKal7 or cKal7. Samples were analyzed in duplicate and probed with Sec14 antibody or Ex1C-peptide antibody. Molecular weights are indicated; GAPDH is a loading control. **C.** Western blots of subcellular fractions from a representative experiment. Equal amounts of protein (10 μg/lane) were probed with the indicated antibodies. Molecular weights are indicated (left). **D.** Samples (500 μg protein from cytosol, P3 and LSM; 250 μg from PSD) were immunoprecipitated with Kal-SR4-7 antibody. 67% of each immunoprecipitate was analyzed by Western blot using Ex1C-peptide antibody and 6.7% was analyzed using Sec14 antibody; amounts were determined after adjusting the amount of recombinant cKal7 loaded to yield signals of similar intensity. A longer exposure of the same gel is shown below. **E.** Using cKal7 recombinant protein as calibrator for each gel set, results of 5 experiments as in **2D** were combined. The (Ex1C-peptide antibody)/(Sec14 antibody) ratio (0.054±0.010, average ±SEM) was used to determine the percentage of Kal7 with c-front. Plot is a Box-and-Whisker, with box extent 25th to 75th percentiles, horizontal line showing median, and whisker extent showing full range of data (Graphpad Prism6).

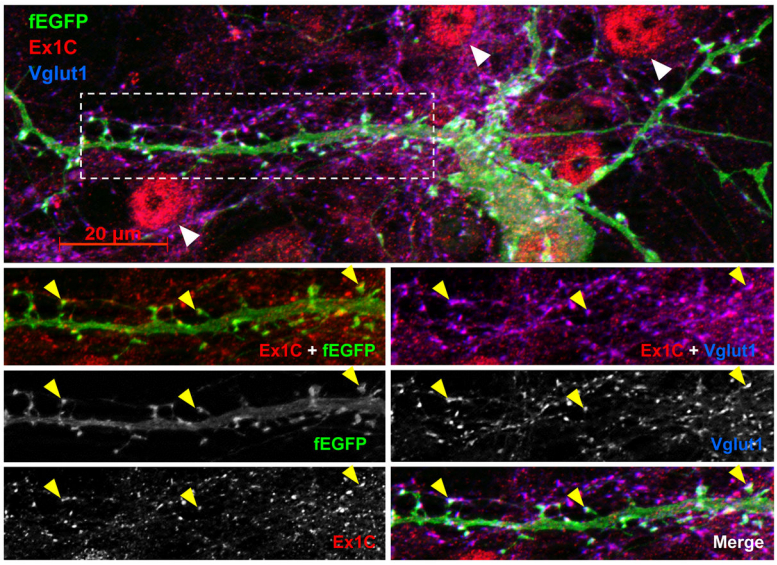

Figure 3. Localization of endogenous cKal to dendritic spines

Rat hippocampal neurons (22 DIV) expressing farnesylated-EGFP (fEGFP) were immunostained with antibodies to Ex1C-peptide (red), Vglut1 (blue) and GFP (green). The representative image shown is a compressed Z-stack, 63X oil objective. Bottom panels show single and double channels of boxed area in top image. Green and red merged image highlights cKal localization to tips of dendritic spines. Red and blue merged image highlights cKal apposition to presynaptic terminals, visualized by Vglut1 staining. Individual channels are shown in grey scale, as indicated. Yellow arrowheads point to discrete spines; white arrowheads point to cell somas; Scale bar, 20 µm.

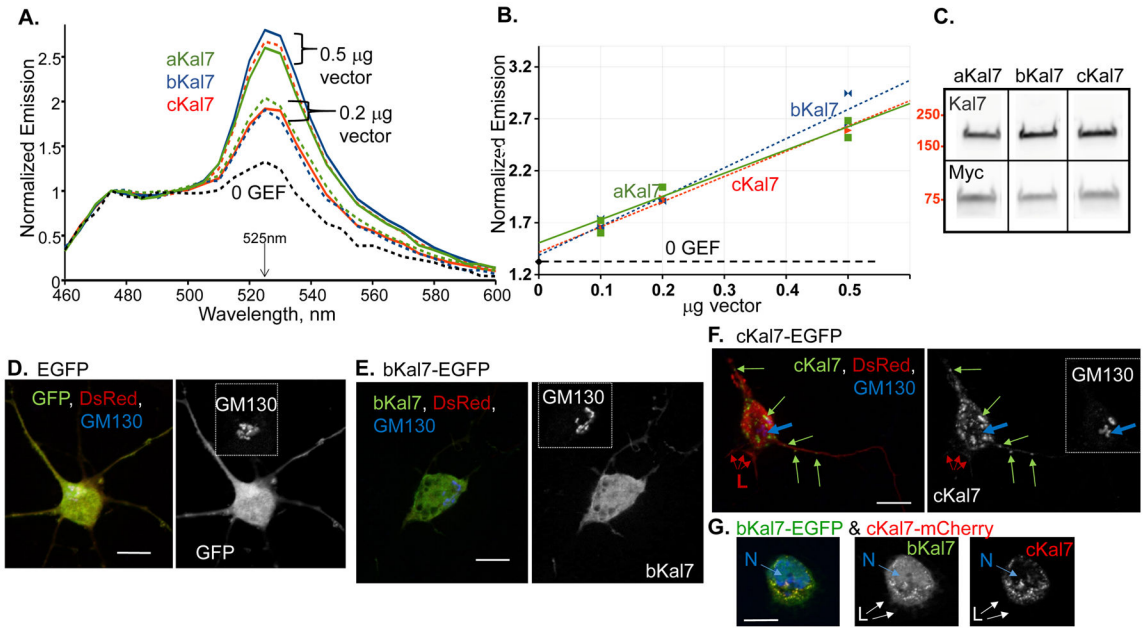

Figure 4. Effect of promoter choice on GEF activity and protein localization

A. Representative emission spectra, with signal intensity normalized to FRET donor emission maximum, 475 nm. Curves are the average of two wells/condition. Dashed-black line, biosensor, no exogenous GEF; data for aKal7 (green), bKal7 (blue) and cKal7 (orange) are shown for 0.2 and 0.5 µg vector. **B.** Group data as FRET ratios (525/475) over amount of transfected DNA for aKal7 (green), bKal7 (blue) and cKal7 (orange) (Least squares best-fit lines). Experiment repeated three times with similar results. **C.** Western blot of cell lysates from representative assay showing equal expression of isoforms (0.5 µg DNA each) and myc-tagged biosensor across groups. Upper panel, Kal7 antibody; lower panel, myc antibody. Rat hippocampal neurons (DIV3) transfected with vectors encoding DsRed and EGFP (**D**), bKal7-EGFP (**E**) or cKal7-EGFP (**F**) were fixed on DIV4. Cultures were stained for GFP (FITC, green) and GM130 (Alexa 633, blue); merged images, GFP alone and GM130 alone are shown. Red L/arrows in Panel **F** mark lamellipodia extending from cell soma; green arrows mark puncta of cKal7-EGFP; blue arrow marks Golgi complex (GM130). **G.** Representative example of bKal7-EGFP and cKal7-mCherry expressed simultaneously in DIV3 rat hippocampal neurons fixed 15 h after transfection; DAPI stain (blue) shows nucleus (N). EGFP and mCherry signals are shown separately; L/arrows mark lamellipodia. All images are a single focal plane, 63X magnification; scale bars, 10 µm.

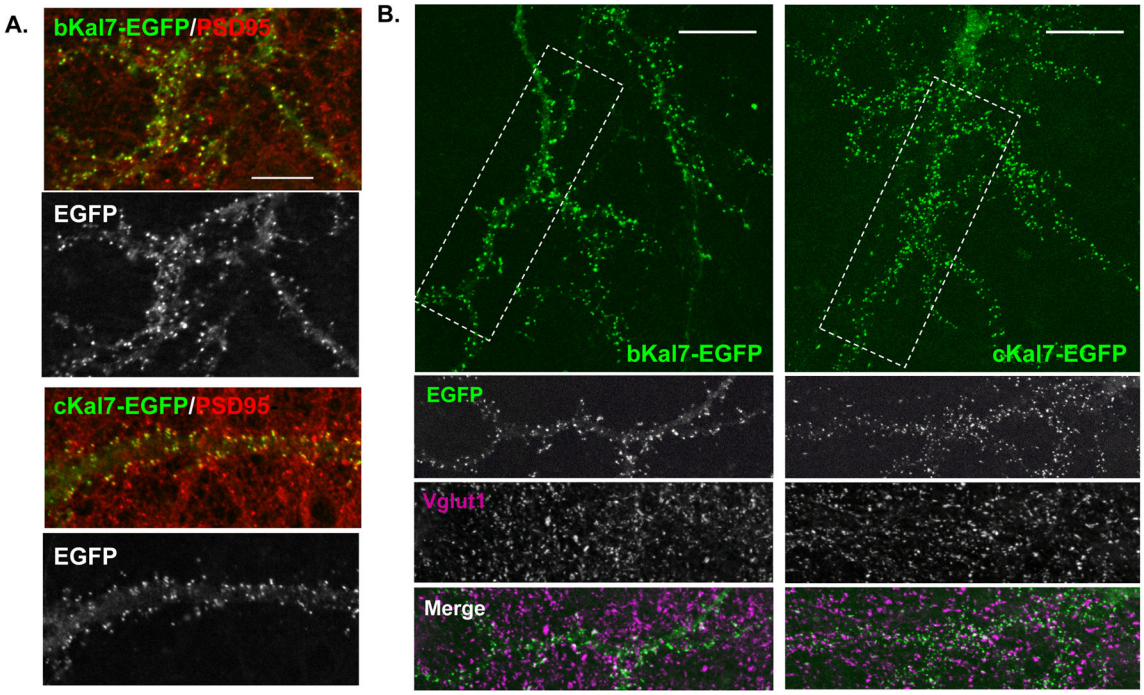

Figure 5. Expression of bKal7-EGFP and cKal7-EGFP in primary neuronal cultures

A. Rat hippocampal neurons, transfected on DIV3 with vectors encoding bKal7-EGFP or cKal7-EGFP, were fixed on DIV17 and stained for EGFP (rat, FITC) and PSD95 (mouse, Cy3). Images are a single focal plane that included both the initial region of the processes and the nucleus; scale bar, 10 μm. **B.** Rat hippocampal neurons transfected with vector encoding either bKal7-EGFP or cKal7-EGFP at DIV2 were fixed and immunostained at DIV15. Images are compressed Z-stacks of 3 focal planes at 63X magnification. Somas were located just above the pictured dendrites. Boxed areas are expanded below with Vglut1 signal shown. Green, GFP; purple, Vglut1, scale bars, 20 μm.

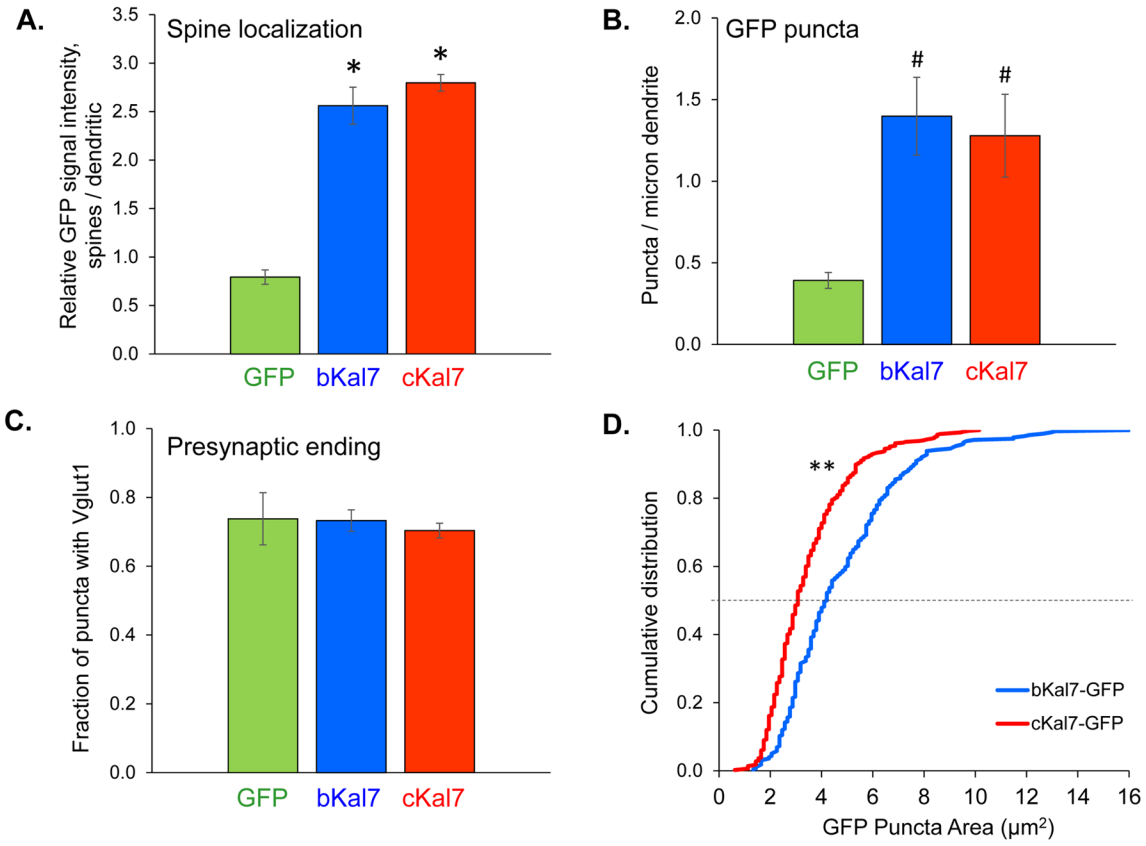

Figure 6. bKal7-EGFP and cKal7-EGFP form GFP puncta that differ in morphology

A. GFP signal intensity was measured following manual identification of spine and dendritic areas. Intensity measurements from multiple areas (≥5 discrete areas for dendrites and dozens for spines) were averaged for each cell. The ratio of spine GFP signal intensity over dendritic shaft GFP signal intensity is displayed as a measure of spine localization. *$p<0.005$ vs. EGFP control. **B.** Linear density of postsynaptic sites was measured by counting GFP puncta (bKal7 and cKal7 conditions) or PSD95 staining (EGFP control cells; not shown). Data are represented as puncta per micron of dendrite. #$p<0.01$ vs. EGFP control. **C.** Quantification showing proportion of postsynaptic puncta (based on GFP or PSD staining, as in **B**) with an apposed Vglut1+ presynaptic ending. **D.** Cumulative distribution plot of postsynaptic GFP-puncta obtained by measuring bKal7-GFP and cKal7-GFP puncta size (276 and 435 individual puncta, respectively); **$p<0.005$ based on Kolmogorov-Smirnov test. Green bars, EGFP; blue, bKal7; orange, cKal7; data are from at least two dendrites from each of 5, 7 and 9 cells for EGFP, bKal7-EGFP and cKal7-EGFP, respectively.

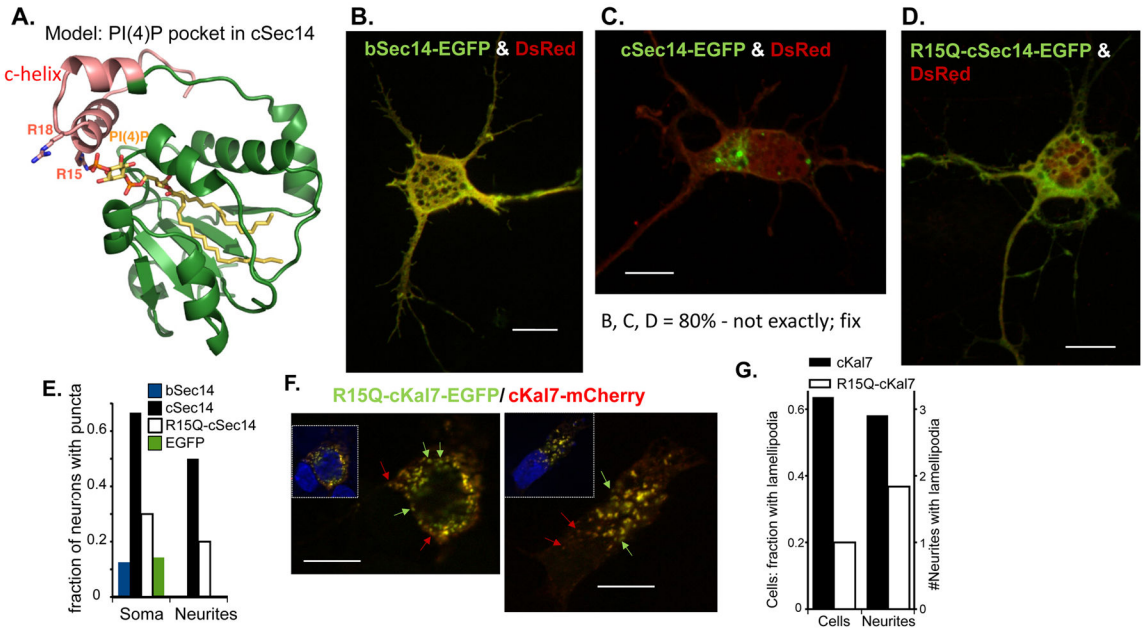

Figure 7. Identification and characterization of key phosphoinositide head group binding site in Ex1C

A. Ribbon diagram of top scoring PHYRE homology model of cSec14 docked with PI(4)P. Predicted Kal-C-Helix is pink. PI(4)P is shown as a yellow stick model located in the presumed binding site. Residues Arg^{15} and Arg^{18}, unique to the Kal-C-Helix, interact with the charged head group of the lipid, forming a lid to the hydrophobic lipid-binding pocket common to the CRAL_TRIO domains of all Sec14 proteins. **B–D.** At DIV3, rat hippocampal neurons were transfected simultaneously with vectors encoding DsRed and EGFP (not shown), bSec14-EGFP (**B**), cSec14-EGFP (**C**) or R15Q-cSec14-EGFP (**D**). Cells were fixed 14 h later; EGFP and DsRed were imaged. **E**. Images (a single focal plane that included processes) were coded and neurons were categorized as having puncta in the cell soma and in their processes. **F**. Rat hippocampal neurons (DIV3) co-transfected with vectors encoding R15Q-cKal7-EGFP and cKal7-mCherry were fixed the next day; nuclei were visualized with DAPI (inset) and merged EGFP and mCherry images are shown. Red arrows note predominantly red puncta; green arrows note predominantly green puncta. Scale bars, 10 μm. **G.** Images of neurons expressing cKal7-EGFP or R15Q-cKal7-EGFP were coded and categorized as having lamellipodia extending from their soma or not (left y-axis); the number of neurites with lamellipodia (per cells) was also quantified (right y-axis).